Rational Design of an Indolebutanoic Acid Derivative as a Novel Aldose Reductase Inhibitor Based on Docking and 3D QSAR Studies of Phenethylamine Derivatives

Won Suck Sun,[†] Yoon Sun Park,[†] Jakyung Yoo,[‡] Ki Duk Park,[†] Sung Han Kim,[†] Jung-Han Kim,[†] and Hyun-Ju Park*[,‡]

Department of Biotechnology, College of Engineering and Bioproducts Research Center, Yonsei University, Seoul 120-749, Korea, and College of Pharmacy, Sungkyunkwan University, Suwon 440-746, Korea

Received November 26, 2002

A series of 45 phenethylamine derivatives were synthesized and evaluated for their inhibitory activity against pig kidney aldose reductase (ALR2, EC 1.1.1.21). Their IC_{50} values ranged from 400 μM to 24 μM. The binding modes of compounds at the active site of ALR2 were examined using flexible docking. The results indicated that phenethylamine derivatives nicely fit into the active pocket of ALR2 by forming various hydrogen bonding and hydrophobic interactions. 3D-QSAR analysis was also conducted using FlexX-docked alignment of the compounds. The best prediction was obtained by CoMSIA combined with hydrophobic and hydrogen bond donor/acceptor field ($q^2 = 0.557$, $r^2 = 0.934$). A new derivative, 4-oxo-4-(4-hydroxyindole)butanoic acid, was designed, taking into account the CoMSIA field and the binding mode derived by FlexX docking. This rationally designed compound exhibits an ALR2 inhibition with an IC_{50} value of 7.4 μM, which compares favorably to that of a well-known ALR2 inhibitor, tolrestat ($IC_{50} = 16$ μM) and represents a potency approximately 240-fold higher than that of an original phenethylamine lead compound, YUA001.

Introduction

Aldose reductase (ALR2, EC 1.1.1.21) is a NADPH-specific aldehyde reductase that catalyzes the conversion of glucose to sorbitol in the polyol pathway and is known to be involved in the onset of long-term diabetic complications such as cataract, neuropathy, retinopathy, and nephropathy.[1−3] To date, studies to develop aldose reductase inhibitors (ARIs) to prevent those complications have yielded many structually diverse ARIs such as tolrestat, sorbinil, zopolrestat, and others.[4−9]

ALR2 contains a $(\alpha/\beta)_8$ barrel motif with a large hydrophobic pocket, approximately 4 × 15 Å wide and 15 Å deep, which favors aromatic and apolar substrates over highly polar monosaccharides. The cofactor NADPH is bound in an extended conformation across the barrel with the nicotinamide ring centered at the bottom of this cavity. Crystal structures of ALR2 complexed with NADPH and diverse ARIs revealed that this pocket is the only possible active site and is mainly composed of two regions: an anion binding site of hydrophilic residues (Tyr48, His110, Trp111, and the 4-*pro*-*R* hydrogen of the nicotineamide ring of NADPH) and a wall of hydrophobic residues (Trp20, Trp79, Trp111, Phe122, Leu300, etc.).[10−13] Many studies have proposed the requisite properties of ARIs: (1) an aromatic ring system to form hydrophobic or $\pi-\pi$ stacking interactions with the hydrophobic amino acid residues in the active site, and (2) ionizable groups such as carboxylic acids and spirohydantoins which can anchor the anionic binding site.[14−16]

Since the early 1980s, along with progress in computer technology, a significant advance has been made in the application of computer modeling to medicinal chemistry.[17−19] Although the predictive power of molecular modeling remains controversial, this methodology has proven useful in drug discovery and recently provides an alternative, so-called virtual screening. Virtual screening is a computing technology to analyze large databases of chemicals in order to discover possible drug candidates, and complement current advances in high-throughput chemical synthesis and biological assays.[20−24] Recently, Costantino et al. reported a series of benzopyran-4-one derivatives as ARIs on the basis of binding mode, and enhanced their activity through SAR study.[25,26] Rastelli et al. identified candidate ARIs having novel pharmacophoric groups such as sulfonic acids, nitro derivatives, sulfonamides, and carbonyl derivatives by performing database search and docking.[27] Iwata et al. also discovered a series of indole-3-acetic acids analogues as ARIs by screening the 3D chemical database (ACD3D).[28]

In our previous study, derivatives (**1**−**11** in Figure 1) of YUA001 (*N*-2-methylbutanoyl tyramine from alkalophilic *Corynebacterium* sp. YUA25) were synthesized and evaluated for their inhibitory activity against pig kidney ALR2. Most of them showed more potent inhibitory activity than that of YUA001; however, the need for enhancing their activity and elucidating their inhibitory mechanism remained.[29]

In this study, we synthesized 45 phenethylamine derivatives and evaluated their inhibitory activity against ALR2. Then, a structure-based drug design approach was taken to find new derivatives with improved activity.[30−33] Flexible docking and 3D-QSAR/CoMSIA

* Corresponding author. Tel.: 82-31-290-7719. Fax: 82-31-290-5403. e-mail: hyunju@skku.ac.kr.
[†] Yonsei University.
[‡] Sungkyunkwan University.

10.1021/jm0205346 CCC: $25.00
Published on Web 11/20/2003

A.

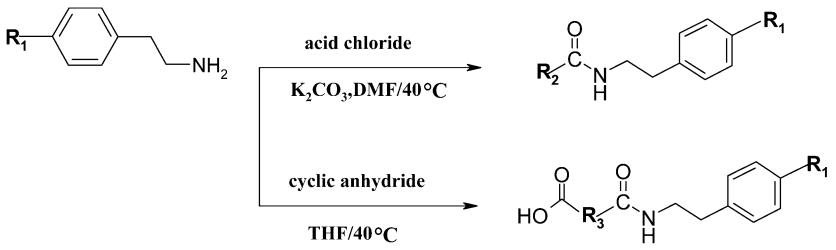

	R_1	R_2	R_3		R_1	R_2	R_3		R_1	R_2	R_3		R_1	R_2	R_3
1	-OH	$-CH_3$		**9**	-OH		$-CH_2CH_2-$	**16**	$-OCH_3$		$-CH_2CH_2-$	**24**	-Cl		$-CH_2CH_2-$
2	-OH	$-(CH_2)_3CH_3$		**10**	-OH		-CH=CH-	**17**	$-OCH_3$		-CH=CH-	**25**	-Cl		-CH=CH-
3	-OH	$-(CH_2)_6CH_3$		**11**	-OH			**18**	$-OCH_3$			**26**	-Cl		
4	-OH	$-(CH_2)_8CH_3$		**12**	-H		$-CH_2CH_2-$	**19**	$-OCH_3$		$-(CH_2)_3-$	**27**	-Cl		$-(CH_2)_3-$
5	-OH	$-(CH_2)_{10}CH_3$		**13**	-H		-CH=CH-	**20**	-F		$-CH_2CH_2-$	**28**	-Br		$-CH_2CH_2-$
6	-OH	$-(CH_2)_{14}CH_3$		**14**	-H			**21**	-F		-CH=CH-	**29**	-Br		-CH=CH-
7	-OH			**15**	-H		$-(CH_2)_3-$	**22**	-F			**30**	-Br		
8	-OH							**23**	-F		$-(CH_2)_3-$	**31**	-Br		$-(CH_2)_3-$

B.

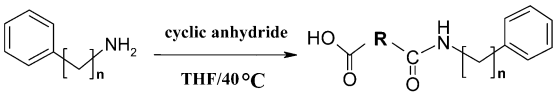

	n	R		n	R
32	*0*	$-CH_2CH_2-$	**36**	*1*	$-CH_2CH_2-$
33	*0*	-CH=CH-	**37**	*1*	-CH=CH-
34	*0*		**38**	*1*	
35	*0*	$-(CH_2)_3-$	**39**	*1*	$-(CH_2)_3-$

C.

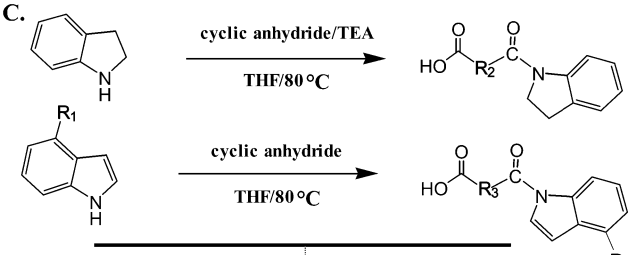

	R_1	R_2	R_3		R_1	R_2	R_3
40		$-CH_2CH_2-$		**43**	H		$-CH_2CH_2-$
41		-CH=CH-		**44**	H		-CH=CH-
42				**45**	H		
				46	OH		$-CH_2CH_2-$

Figure 1. Preparation of (A) phenethylamine derivatives, **1**−**31**, (B) benzyl and phenylamine derivatives, **32**−**39**, (C) indoline and indole derivatives, **40**−**46**.

analysis were used to explore structure−activity relationships of the compounds we identified, and guided the design of the most potent derivative, 4-oxo-4-(4-hydroxyindole)butanoic acid (**46** in Figure 1). The present study demonstrates a successful example of rational drug design approaches: we used not only a CoMSIA model to decide the substituent properties of a new derivative, but also a binding conformation obtained from flexible docking analysis to define positions to be substituted.

Results

Synthesis and Biochemical Evaluation. A novel aldose reductase inhibitor, *N*-[2-(4-hydroxyphenyl)ethyl]-2-methylbutanamide (YUA001), isolated from alkalophilic *Corynebacterium sp.* YUA25,[29] was chosen as a lead, and various structural modifications were conducted to find new synthetic derivatives with improved activities. We modified it with an elongated aliphatic chain (**1**−**6**) and the introduction of aromatic rings (**7**−**8**) or terminal carboxyl acids (**9**−**45**), while maintaining phenethylamine as a framework. The syntheses of *N*-substituted tyramine derivatives **1**−**11** were reported previously.[34,35] As outlined in Figure 1A and B, the para-substituted tyramine derivatives **12**−**31** were prepared by treating each anhydride with para-substituted amine in acetonitrile (THF) at 40 °C. For benzyl and phenylamine derivatives **32**−**39**, cyclic anhydride was reacted

Table 1. Inhibitory Activities against Pig Kidney Aldose Reductase of Phenethylamine Derivatives **1**−**46**

compounds	IC_{50} value (M)[a]	compounds	IC_{50} value (M)[a]
YUA001	1.8×10^{-3}	**24**	0.99×10^{-4}
1	1.6×10^{-4}	**25**	1.12×10^{-4}
2	1.3×10^{-4}	**26**	2.03×10^{-4}
3	1.2×10^{-4}	**27**	1.54×10^{-4}
4	1.1×10^{-4}	**28**	0.94×10^{-4}
5	1.1×10^{-4}	**29**	0.99×10^{-4}
6	1.5×10^{-4}	**30**	0.81×10^{-4}
7	1.6×10^{-4}	**31**	1.1×10^{-4}
8	1.0×10^{-4}	**32**	1.92×10^{-4}
9	3.9×10^{-4}	**33**	1.82×10^{-4}
10	0.8×10^{-4}	**34**	2.27×10^{-4}
11	3.4×10^{-4}	**35**	4.4×10^{-4}
12	0.78×10^{-4}	**36**	1.41×10^{-4}
13	0.73×10^{-4}	**37**	1.5×10^{-4}
14	0.88×10^{-4}	**38**	1.8×10^{-4}
15	1.04×10^{-4}	**39**	1.33×10^{-4}
16	1.7×10^{-4}	**40**	1.02×10^{-4}
17	1.55×10^{-4}	**41**	0.4×10^{-4}
18	1.77×10^{-4}	**42**	0.95×10^{-4}
19	1.85×10^{-4}	**43**	0.24×10^{-4}
20	0.94×10^{-4}	**44**	0.37×10^{-4}
21	0.75×10^{-4}	**45**	0.3×10^{-4}
22	0.88×10^{-4}	**46**	0.74×10^{-5}
23	0.76×10^{-4}	Tolrestat[b]	0.16×10^{-4}

[a] Evaluted in vitro against pig kidney aldose reductase. [b] *N*-[[6-Methoxy-5-(trifluoromethyl)-1-naphthalenyl]thioxomethyl]-*N*-methylglycine.

with benzyl or phenylamine for 10 h at 40 °C. The indoline and indole derivatives **40**−**46** were synthesized following the synthetic method shown in Figure 1C. The anhydrides were treated with indoline and indole in the presence of a large excess of triethylamine and vigorously stirred for 24 h at 80 °C.

The inhibitory activities of the compounds (**1**−**45**) against ALR2 are evaluated and expressed as IC_{50} values in Table 1. Various modifications of phenethyl, phenyl, and benzylamine (**1**−**39**) did not improve the inhibitory activity significantly, exhibiting IC_{50} values in the low millimolar to micromolar range. However, replacement of the phenethylamine unit with indole or indoline ring (**40**−**45**) increased the activity significantly. Notably, 4-oxo-4-indolebutanoic acid (**43**) exhibited the strongest ALR2 inhibitory activity with an IC_{50} value of 24 μM, which is comparable to the activity of tolrestat (IC_{50} = 16 μM).

Docking Study. We conducted docking analysis using the FlexX algorithm[36,37] not only to examine the binding mode of the compounds at the active site of aldose reductase (AR), but also to obtain a basis for further synthetic derivatization. The crystal structure of the ternary complex which includes cofactor NADPH and tolrestat was used in this study (pdb entry = 1AH3).[38] A COOH hydrophilic head of tolrestat and the compounds **9**−**45** (pK_a between 3.5 and 5.0) is probably bound by AR in the form of carboxylate anion; the COOH group of those molecules was calculated in the anionic form which shares a negative charge between two oxygen atoms. The energy-minimized structure of tolrestat was preliminarily docked into ALR2 to examine how closely the FlexX algorithm can reproduce the experimentally determined binding conformation of tolrestat at the active site of AR. A superposition of docked tolrestat onto the crystallographic geometry yielded a root-mean-square (rms) deviation of 0.74 Å and revealed that FlexX was successful in reproducing the binding conformation of tolrestat.

To evaluate the relationship between relative ALR2 inhibitory activities and binding energy scores obtained from FlexX docking, we have used consensus scoring program, Cscore, that integrates multiple well-known scoring functions: a GOLD-like function, a DOCK-like function, ChemScore, a PMF function, and FlexX.[39−42] The FlexX scoring function performs best, and the resulting ranking showed good agreement with the ALR2 inhibitory activities of the compounds. Therefore, we selected the top-scoring conformer of each ligand based on the FlexX scores calculated from FlexX, and positioned it onto the active site of ALR2. They fit well into the active site pocket of ALR2 occupied by tolrestat in the X-ray crystal structure. All the compounds primarily contain either a phenolic hydroxyl (YUA001 and **1**−**8**) or carboxylate (**9**−**45**) group. Those groups anchor into the anionic binding site by forming numerous hydrogen bonds with $NADP^+$ or the side chain of Trp111, His110, and Tyr48. The interaction between the ligand and amino acid residues of the active site were determined and are illustrated in Figure 2 for the three representative compounds, YUA001, **10**, and **43**, in comparison with the X-ray structure of tolrestat.[38] An aliphatic chain of the acyl moiety of YUA001 is positioned close to Phe122 and Leu300, possibly forming a hydrophobic interaction. For compound **10**, the phenolic hydroxyl group forms additional hydrogen bonding with the Ser302 residue. The indole moiety of compound **43** intercalates between Phe122 and Leu300 and is likely to play an important role in enhancing the affinity in the active site through the $\pi-\pi$ interaction.

3D-QSAR/CoMSIA Modeling. 3D-QSAR methods, especially CoMFA(Comparative Molecular Field Analysis),[43] are used widely in drug design, because they allow rapid generation of QSARs from which biological activity of newly designed molecules can be predicted. The basic assumption in CoMFA is that an appropriate sampling of the steric and electrostatic fields around a set of aligned molecules might provide all the information necessary for understanding their biological activities. A main difficulty in the application of 3D-QSAR methods such as CoMFA is that a spatial orientation of the ligands toward one another has to be found to yield a correct model. Therefore, the success of molecular field analysis largely determined by the quality of alignment of studied molecules. Another 3D-QSAR method, the CoMSIA (Comparative Molecular Similarity Indices Analysis)[44,45] technique, is recently of particular interest since it is less alignment-sensitive than CoMFA and includes a hydrophobic field and two hydrogen bond fields. In this study, we performed 3D-QSAR by CoMSIA on a select 42 compounds (except compound **46** in Table 2), by using hydrophobicity and hydrogen bond donor and acceptor as descriptors and attempted to obtain a reliable CoMSIA model to guide to the design of analogous AR inhibitors. For alignment of the ligands, we used a superimposition of the top-scoring conformations derived from FlexX docking.[46] As listed in Table 2, the biological activities of 42 ligands used for the 3D-QSAR study were expressed as pIC_{50} values. To derive a predictive relationship model, the partial least squares (PLS) method was used, and the

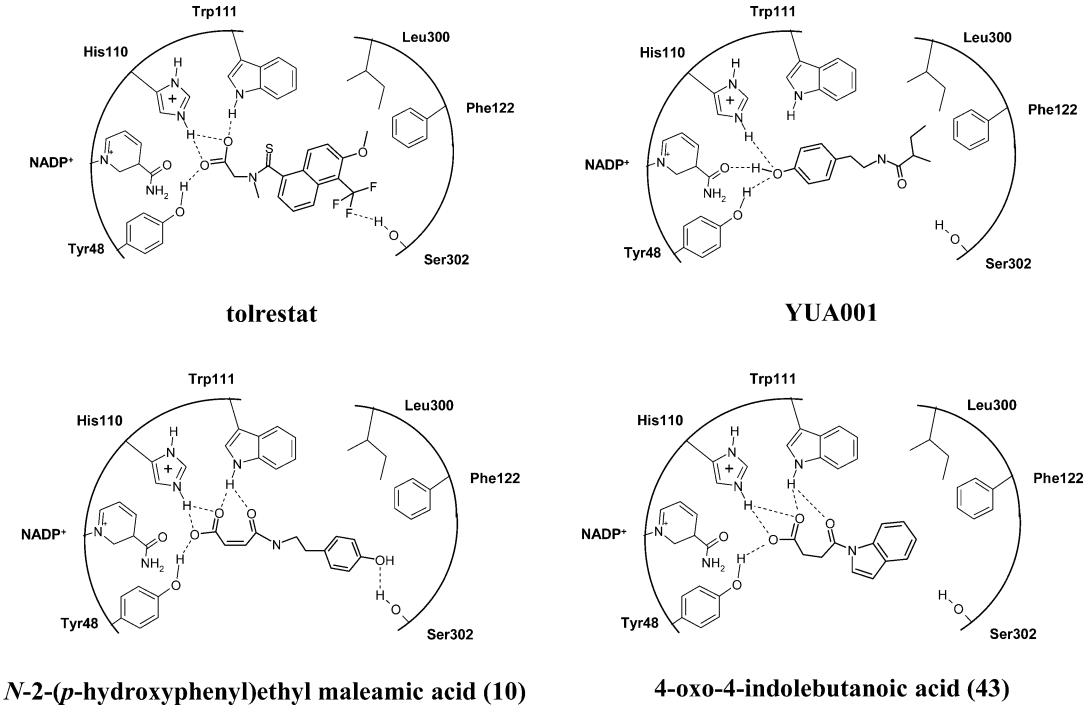

Figure 2. Binding modes of phenethylamine derivatives obtained from the FlexX docking. Dotted lines indicate hydrogen bonding interactions (<2.0 Å).

analysis was conducted by correlating variations in the ligands' biological activities with variations in their CoMSIA fields. A correlation coefficient of $r^2 = 0.934$ and a cross-validated coefficient of $q^2 = 0.557$ were obtained (Table 3). These results indicate a good predictive ability of the model. This is also reflected by the small deviation of the calculated from the experimental values of IC_{50} (Table 2).

Design Based on 3D-QSAR and Docking. Analysis of CoMSIA contour maps (Figure 3) revealed that hydrogen bond donor-favored region exists around 4-position, and hydrophobicity-disfavored region around the 5- and 6- of indole moiety of the most potent compound, **43**. On the basis of this observation, we built three modified structures containing a hydroxyl group at 4-, 5-, or 6-position of the indole ring, respectively. Then, FlexX docking was conducted for the modified structures, and resulting docked conformations were examined to identify favorable interactions with ALR2. As demonstrated in Figure 4, the analogue with a hydroxyl group at the 4-position of the indole ring (compound **46**) yielded the best agreement with the ALR2-bound conformation of tolrestat. In particular, 4-OH of **46** is superimposed onto the trifluoro group of tolrestat, which forms a hydrogen bond with the OH group of Ser 302 in the X-ray structure. In the docked structure of **46**:ALR2 complex, the distance between two oxygen atoms in 4-OH of **46** and the OH of Ser 302 is 1.4 Å, which is reasonable for the formation of a strong hydrogen bond. In addition, the pIC_{50} value of **46** predicted by the CoMSIA model is 5.036 (Table 2), which is higher than the activity of tolrestat ($pIC_{50} = 4.796$). Compound **46** was synthesized and tested for ALR2 inhibitory activity in comparison with tolrestat. The IC_{50} value of **46** was 7.4 μM, which is superior to that of both tolrestat ($IC_{50} = 16$ μM) and the lead compound, **43** ($IC_{50} = 24$ μM). Thus, compound **46**, which was built taking into account the CoMSIA field and the binding mode derived by FlexX docking, is a 243-fold more potent inhibitor than YUA001, a mother compound of this study.

Conclusions

In this study, our laborious synthetic efforts (up to compound **45** starting from phenylethylamine derivative YUA001) yield AR inhibitors with IC_{50} values in the range of 1.8 mM to 24 μM, and also indicated that indole butanoic acid (compound **43**) as a scaffold would have the most potent activity. Therefore, we rationally designed compound **46**, a simple synthetic analogue of lead compound **43**, based upon the results obtained from FlexX docking and 3D-QSAR/CoMSIA analysis. Compound **46** exhibited improved activity in comparison with compound **43**, and 243-fold higher inhibitory activity than YUA001. Further improvement of potency would be achieved in future investigation using compound **46** as a new lead. Our study demonstrates the efficiency of computer-based drug design tools not only for understanding the molecular basis of drug−receptor interaction, but also for the discovery and further optimization of new leads.

Experimental Section

Apparatus and Reagents. Spectra of ^{1}H NMR were recorded on Varian UNITY 300 (Palo Alto, CA). The ESI mass spectra were recorded with a Fison-VG platform (Beverly, MA). UV spectrophotometer (Shimadzu, UV120) was used for aldose reductase inhibitory activity assay at 340 nm. Computer modeling was performed with Tripos Sybyl 6.8[47] in SGI Octane II. Reagents and solvents for the synthesis of phenetylamine derivatives (indole, indoline, etc.) were purchased from Sigma-Aldrich Chemical Co. (St. Louis, MO). TLC was performed on Merck Kiesel 60 F254 plates (Darmstadt, Germany). Merck Kiesel 60 (Darmstadt, Germany) was used for column chromatography.

Table 2. Residuals of the Calculated Activities Derived from the CoMSIA Model

compounds	pIC_{50}* [a]	hydrophobic[b]	donor[c]	acceptor[d]	Pre-pIC_{50}[e]	residual[f]
YUA001	2.745	4.65	1.97	2.28	2.813	−0.0683
1	3.959	3.59	1.98	2.64	3.839	0.1196
2	3.886	4.7	1.13	2.64	3.938	−0.0519
3	3.921	5.55	1.15	2.65	3.845	0.0758
7	3.796	4.66	2	2.65	3.765	0.0309
8	4.000	3.74	1.96	2.32	4.044	−0.044
9	4.108	4.04	1.96	4.97	4.154	−0.0461
10	4.097	3.91	1.96	4.93	4.118	−0.0211
11	3.469	4.97	1.97	4.91	3.326	0.1425
12	4.108	4.37	1.59	4.85	3.999	0.1089
13	4.137	4.25	1.59	5.03	4.059	0.0777
14	4.056	4.98	1.59	4.94	3.998	0.0575
15	3.983	4.61	1.61	4.11	3.933	0.05
16	3.770	3.92	1.59	5.12	3.88	−0.1104
17	3.807	3.83	1.59	5.03	3.952	−0.1453
18	3.752	4.66	1.59	5.19	3.833	−0.081
19	3.733	4.15	1.59	4.47	3.673	0.0598
20	4.027	4.54	1.59	4.85	4.008	0.0189
21	4.125	4.46	1.59	5.03	3.974	0.1509
22	4.056	5.07	1.59	4.62	4.103	−0.0475
23	4.119	4.78	1.59	4.36	3.959	0.1602
24	4.004	5.19	1.59	4.85	4.018	−0.0136
25	3.951	5.15	1.59	5.03	3.988	−0.0372
26	3.693	5.76	1.59	4.63	3.891	−0.1985
27	3.813	5.46	1.61	4.36	3.945	−0.1325
28	4.027	5.78	1.59	4.85	4.026	0.0009
29	4.004	5.65	1.59	4.45	4.087	−0.0826
30	4.092	6.34	1.59	4.63	3.939	0.1525
31	3.959	5.91	1.59	4.84	4.048	−0.0894
32	3.717	3.47	1.6	4.79	3.633	0.0837
33	3.740	3.32	1.6	4.52	3.7	0.0399
34	3.644	4.3	1.6	4.2	3.575	0.069
35	3.357	3.74	1.59	4.4	3.479	−0.1225
36	3.851	4.02	1.59	4.21	3.907	−0.0562
37	3.824	3.87	1.59	4.06	3.805	0.0189
39	3.876	4.23	1.61	4.18	3.936	−0.0599
40	3.991	3.74	0	4.87	4.189	−0.1976
41	4.398	3.6	0	4.65	4.236	0.1619
42	4.022	3.95	0	4.46	4.043	−0.0207
43	4.620	3.6	0	4.85	4.629	−0.0092
45	4.523	3.81	0	4.47	4.504	0.0189
tolrestat	4.796	6.08	0	3.62	4.851	−0.0551
46	5.131	3.37	1.17	4.98	5.036	0.0947

[a] pIC_{50}* = −log IC_{50}. [b] Hydrophobicity. [c] Hydrogen bond donor. [d] Hydrogen bond acceptor fields. [e] Predicted pIC_{50}. [f] pIC_{50} − Predicted pIC_{50}.

Table 3. Summary of CoMSIA Results

	CoMSIA
optimum number of components	5
probe atom	C sp^3
cross-validated r^2 (q^2)	0.557
standard error of estimate (S)	0.102
conventional r^2	0.934
F-value	105.508
relative contributions	
hydrophobicity	43.0%
hydrogen donor	22.1%
hydrogen acceptor	34.9%

Aldose Reductase Inhibitory Activity. The preparation of AR and In vitro AR inhibition assays were conducted according to the method in a previous publication.[34] Tolrestat was used as positive control.

General Procedure for the Synthesis of Para-Substituted Penethylamine Derivatives (12−31). Appropriate anhydride (succinic, maleic, phthalic, and glutaric anhydride; 1.5 equiv) was added to para-substituted amine relatively in acetonitrile at room temperature. The mixture was stirred for 10 h at 40 °C and concentrated. The residual oil was chromatographed on silica gel ($CHCl_3$:MeOH = 9:1) and washed with ether to give **12**−**31**.

General Procedure for the Synthesis of Benzyl and Phenylamine Derivatives (32−39). Each benzyl and phenylamine was reacted with cyclic anhydrides, such as succinic, maleic, phthalic, and glutaric anhydride (1.5 equiv) in acetonitrile at room temperature, followed by stirring for 10 h in 40 °C. The concentrated residual was further purified with silica gel column chromatography ($CHCl_3$:MeOH = 9:1) to give **32**−**39**.

General Procedure for the Synthesis of Indoline and Indole Derivatives (40−46). The reaction mixture of the required indole or indoline, appropriate anhydrides (1.5 equiv) and TEA (10 equiv) in acetonitrile was refluxed overnight. After evaporation of solvent, residue was purified by silica gel chromatography ($CHCl_3$:MeOH = 20:1) and washed with hexane to give **40**−**46**.

***N*-2-Phenylethylsuccinamic Acid (12).** The mixture of succinic anhydride (262 mg, 2.62 mmol) and phenethylamine (265 mg, 2.19 mmol) in acetonitrile (30 mL) gave **12** (513 mg, 64%): ^{1}H NMR (DMSO-d_6, 300 MHz) δ 7.92 (1H, t, N*H*CH_2-CH_2Ar), δ 7.32 (1H, m, Ar-*H*), δ 7.15 (4H, m, Ar-*H*), δ 3.22 (2H, m, NHC*H*$_2$$CH_2$Ar), δ 2.7 (2H, t, NHCH_2C*H*$_2$Ar), δ 2.41 (2H, t, COC*H*$_2$$CH_2$COOH), δ 2.32 (2H, t, COCH_2C*H*$_2$COOH); ESI-MS m/z 221 (M^+). Anal. ($C_{12}H_{15}NO_3$) C, H, N.

***N*-2-Phenylethylmaleamic Acid (13).** The mixture of maleic anhydride (256 mg, 2.62 mmol) and phenethylamine (265 mg, 2.19 mmol) in acetonitrile (30 mL) gave **13** (478 mg, 60%): ^{1}H NMR (DMSO-d_6, 300 MHz), δ 6.49 (3H, d, Ar-*H*), δ 6.48 (2H, d, Ar-*H*), δ 6.39 (1H, t, COC*H* = CHCOOH), δ 6.29 (1H, t, COCH=C*H*COOH), δ 3.41 (2H, m, NHC*H*$_2$$CH_2$Ar), δ

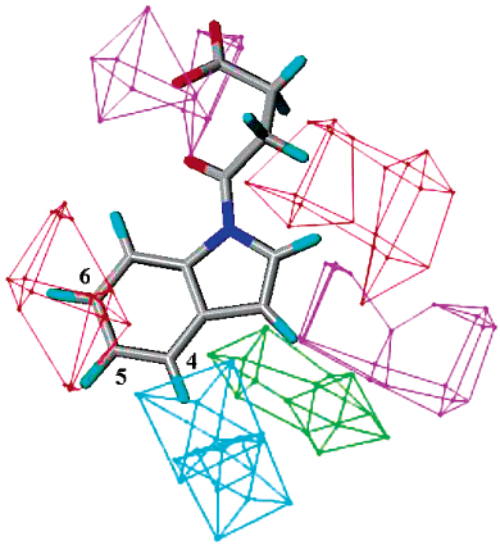

	Favored	Disfavored
Hydrophobic field	Blue	Red
Hydrogen donor	Cyan	Yellow
Hydrogen acceptor	Magenta	Green

Figure 3. CoMSIA hydrogen bonding donor/acceptor and hydrophobic contour plots of 4-oxo-4-indolebutanoic acid (**43**). Cyan polyhedra indicate regions where hydrogen bonding donor groups will enhance the binding. Magenta polyhedra indicate regions where hydrogen bonding acceptor will enhance the affinity. Red polyhedra indicate where hydrophilic groups increase the binding.

2.46 (2H, t, NHCH$_2$C*H*$_2$Ar); ESI-MS *m*/*z* 219 (M^+). Anal. ($C_{12}H_{13}NO_3$) C, H; N: calcd, 6.33; found, 6.43.

***N*-2-Phenylethylphthalamic Acid (14).** The mixture of phthalic anhydride (390 mg, 2.62 mmol) and phenethylamine (265 mg, 2.19 mmol) in acetonitrile (30 mL) gave **14** (345 mg, 35%): ^{1}H NMR (DMSO-d_6, 300 MHz) δ 8.4 (1H, d, N*H*CH$_2$-CH$_2$Ar), δ 7.75 (2H, m, CO*Ph*COOH), δ 7.4 (1H, d, CO*Ph*-COOH), δ 7.3 (5H, m, Ar-*H*), δ 3.54 (2H, m, NHC*H*$_2$CH$_2$Ar), δ 2.71 (2H, t, NHCH$_2$C*H*$_2$Ar); ESI-MS *m*/*z* 269 (M^+). Anal. ($C_{16}H_{15}NO_3$) C, H; N: calcd, 5.20; found, 5.15.

***N*-2-Phenylethylglutaramic Acid (15).** The mixture of glutaric anhydride (299 mg, 2.62 mmol) and phenethylamine (265 mg, 2.19 mmol) in acetonitrile (30 mL) gave **15** (304 mg, 36%): ^{1}H NMR (DMSO-d_6, 300 MHz) δ 7.87 (1H, t, N*H*CH$_2$-CH$_2$CH$_2$Ar), δ 6.89 (3H, m, Ar-*H*), δ 6.73 (2H, dd, Ar-*H*), δ 3.16 (2H, m, NHC*H*$_2$CH$_2$Ar), δ 2.65 (2H, t, NHCH$_2$C*H*$_2$Ar), δ 2.16 (2H, m, COC*H*$_2$CH$_2$CH$_2$COOH), δ 2.01 (1H, m, COCH$_2$CH$_2$C*H*$_2$-COOH), δ 1.52 (1H, m, COCH$_2$C*H*$_2$CH$_2$COOH); ESI-MS *m*/*z* 235 (M^+). Anal. ($C_{13}H_{17}NO_3$) C; H: calcd, 7.28; found, 7.32, N: calcd, 5.95; found, 5.90.

***N*-2-(*p*-Methoxyphenyl)ethylsuccinamic Acid (16).** The mixture of succinic anhydride (262 mg, 2.62 mmol) and (*p*-methoxyphenyl)ethylamine (330 mg, 2.19 mmol) in acetonitrile (30 mL) gave **16** (377 mg, 41%): ^{1}H NMR (DMSO-d_6, 300 MHz) δ 7.89 (1H, t, N*H*CH$_2$CH$_2$Ar), δ 7.11 (2H, d, Ar-*H*), δ 6.83 (2H, d, Ar-*H*), δ 3.70 (3H, s, OC*H*$_3$), δ 3.20 (2H, m, NHC*H*$_2$CH$_2$Ar), δ 2.59 (2H, t, NHCH$_2$C*H*$_2$Ar), δ 2.40 (2H, t, COC*H*$_2$CH$_2$COOH), δ 2.27 (2H, t, COCH$_2$C*H*$_2$COOH); ESI-MS *m*/*z* 251 (M^+). Anal. ($C_{13}H_{17}NO_4$) C; H: calcd, 6.82; found, 6.95, N: calcd, 5.57; found, 5.54.

***N*-2-(*p*-Methoxyphenyl)ethylmaleamic Acid (17).** The mixture of maleic anhydride (256 mg, 2.62 mmol) and (*p*-methoxyphenyl)ethylamine (330 mg, 2.19 mmol) in acetonitrile (30 mL) gave **17** (176 mg, 19%): ^{1}H NMR (DMSO-d_6, 300 MHz) δ 9.13 (1H, t, N*H*CH$_2$CH$_2$Ar), δ 7.14 (2H, d, Ar-*H*), δ 6.86 (2H, d, Ar-*H*), δ 6.38 (1H, d, COC*H* = CHCOOH), δ 6.23 (1H, d, COCH=C*H*COOH), δ 3.72 (3H, s, OC*H*$_3$), δ 3.4 (2H, m, NHC*H*$_2$CH$_2$Ar), δ 2.72 (2H, t, NHCH$_2$C*H*$_2$Ar); ESI-MS *m*/*z* 249 (M^+). Anal. ($C_{13}H_{15}NO_4$) C; H: calcd, 6.07; found, 6.19, N: calcd, 5.62; found, 5.71.

***N*-2-(*p*-Methoxyphenyl)ethylphthalamic Acid (18).** The mixture of phthalic anhydride (390 mg, 2.62 mmol) and (*p*-methoxyphenyl)ethylamine (330 mg, 2.19 mmol) in acetonitrile (30 mL) gave **18** (276 mg, 25%): ^{1}H NMR (DMSO-d_6, 300 MHz) δ 8.37 (1H, t, N*H*CH$_2$CH$_2$Ar), δ 7.75 (1H, d, CO*Ph*COOH), δ 7.65 (2H, m, CO*Ph*COOH), δ 7.18 (1H, m, CO*Ph*COOH), δ 7.16 (2H, d, Ar-*H*), δ 6.86 (2H, d, Ar-*H*), δ 3.72 (3H, s, OC*H3*), δ 2.73 (2H, m, NHC*H2*CH2Ar), δ 2.49 (2H, t, NHCH2C*H2*Ar); ESI-MS *m*/*z* 299 (M^+). Anal. ($C_{17}H_{17}NO_4$) C; H: calcd, 5.72; found, 5.68, N: calcd, 4.68; found, 4.63.

***N*-2-(*p*-Methoxyphenyl)ethylglutaramic Acid (19).** The mixture of glutaric anhydride (299 mg, 2.62 mmol) and (*p*-methoxyphenyl)ethylamine (330 mg, 2.19 mmol) in acetonitrile (30 mL) gave **19** (316 mg, 33%): ^{1}H NMR (DMSO-d_6, 300 MHz) δ 7.84 (1H, t, N*H*CH$_2$CH$_2$Ar), δ 7.1 (2H, d, Ar-*H*), δ 6.83 (2H, dd, Ar-*H*), δ 3.71 (3H, s, OC*H*$_3$), δ 3.18 (2H, m, NHC*H*$_2$CH$_2$-Ar), δ 2.61 (2H, t, NHCH$_2$C*H*$_2$Ar), δ 2.17 (2H, m, COC*H*$_2$CH$_2$-CH$_2$COOH), δ 2.07 (2H, m, COCH$_2$CH$_2$C*H*$_2$COOH), δ 1.69 (2H, m, COCH$_2$C*H*$_2$CH$_2$COOH); ESI-MS *m*/*z* 265 (M^+). Anal. ($C_{14}H_{19}$-NO_4) C; H: calcd, 7.22; found, 7.28, N: calcd, 5.28; found, 5.21.

***N*-2-(*p*-Fluorophenyl)ethylsuccinamic Acid (20).** The mixture of succinic anhydride (262 mg, 2.62 mmol) and (*p*-fluorophenyl)ethylamine (304 mg, 2.19 mmol) in acetonitrile (30 mL) gave **20** (429 mg, 49%): ^{1}H NMR (DMSO-d_6, 300 MHz) δ 7.92 (1H, t, N*H*CH$_2$CH$_2$Ar), δ 7.22 (2H, d, Ar-*H*), δ 7.08 (2H, d, Ar-*H*), δ 3.21 (2H, m, NHC*H*$_2$CH$_2$Ar), δ 2.66 (2H, t, NHCH$_2$C*H*$_2$Ar), δ 2.38 (2H, t, COC*H*$_2$CH$_2$COOH), δ 2.26 (2H, t, COCH$_2$C*H*$_2$COOH); ESI-MS *m*/*z* 239 (M^+). Anal. ($C_{12}H_{14}$-FNO_3) C; H: calcd, 5.90; found, 5.98, N: calcd, 5.85; found, 5.91.

***N*-2-(*p*-Fluorophenyl)ethylmaleamic Acid (21).** The mixture of maleic anhydride (256 mg, 2.62 mmol) and (*p*-fluorophenyl)ethylamine (304 mg, 2.19 mmol) in acetonitrile (30 mL) gave **21** (650 mg, 75%): ^{1}H NMR (DMSO-d_6, 300 MHz), δ 9.12 (1H, t, N*H*CH$_2$CH$_2$Ar), δ 7.25 (2H, d, Ar-*H*), δ 7.10 (2H, d, Ar-*H*), δ 6.36 (1H, t, COC*H* = CHCOOH), δ 6.23 (1H, t, COCH=C*H*COOH), δ 3.37 (2H, m, NHC*H*$_2$CH$_2$Ar), δ 2.76 (2H, t, NHCH$_2$C*H*$_2$Ar); ESI-MS *m*/*z* 237 (M^+). Anal. ($C_{12}H_{12}FNO_3$) C, H; N: calcd, 6.33; found, 6.43.

***N*-2-(*p*-Fluorophenyl)ethylphthalamic Acid (22).** The mixture of phthalic anhydride (390 mg, 2.62 mmol) and (*p*-fluorophenyl)ethylamine (304 mg, 2.19 mmol) in acetonitrile (30 mL) gave **22** (746 mg, 71%**)**: ^{1}H NMR (DMSO-d_6, 300 MHz) δ 8.38 (1H, t, N*H*CH$_2$CH$_2$Ar), δ 7.73 (1H, s, CO*Ph*COOH), δ 7.54 (2H, d, Ar-*H*), δ 7.29 (3H, s, CO*Ph*COOH), δ 7.11 (2H, d, Ar-*H*), δ 3.15 (2H, m, NHC*H*$_2$CH$_2$Ar), δ 2.80 (2H, t, NHCH$_2$C*H*$_2$-Ar); ESI-MS *m*/*z* 287 (M^+). Anal. ($C_{16}H_{14}FNO_3$) C; H: calcd, 4.91; found, 4.87, N: calcd, 5.95; found, 5.90.

***N*-2-(*p*-Fluorophenyl)ethylglutaramic Acid (23).** The mixture of glutaric anhydride (299 mg, 2.62 mmol) and (*p*-fluorophenyl)ethylamine (304 mg, 2.19 mmol) in acetonitrile (30 mL) gave **23** (438 mg, 47%): ^{1}H NMR (DMSO-d_6, 300 MHz) δ 7.86 (1H, t, N*H*CH$_2$CH$_2$Ar), δ 7.21 (2H, d, Ar-*H*), δ 7.08 (2H, dd, Ar-*H*), δ 3.23 (2H, m, NHC*H*$_2$CH$_2$Ar), δ 2.66 (2H, t, NHCH$_2$C*H*$_2$Ar), δ 2.14 (2H, m, COC*H*$_2$CH$_2$CH$_2$COOH), δ 2.04 (2H, m, COCH$_2$CH$_2$C*H*$_2$COOH), δ 1.65 (2H, m, COCH$_2$C*H*$_2$-CH$_2$COOH); ESI-MS *m*/*z* 253 (M^+). Anal. ($C_{13}H_{16}FNO_3$) C, H; N: calcd, 5.53; found, 5.41.

***N*-2-(*p*-Chlorophenyl)ethylsuccinamic Acid (24).** The mixture of succinic anhydride (262 mg, 2.62 mmol) and (*p*-chlorophenyl)ethylamine (340 mg, 2.19 mmol) in acetonitrile (30 mL) gave **24** (213 mg, 23%): ^{1}H NMR (DMSO-d_6, 300 MHz) δ 7.31 (2H, d, Ar-*H*), δ 7.20 (2H, d, Ar-*H*), δ 3.21 (2H, m, NHC*H*$_2$CH$_2$Ar), δ 2.66 (2H, t, NHCH$_2$C*H*$_2$Ar), δ 2.40 (2H, t, COC*H*$_2$CH$_2$COOH), δ 2.25 (2H, t, COCH$_2$C*H*$_2$COOH); ESI-MS *m*/*z* 255 (M^+). Anal. ($C_{12}H_{14}ClNO_3$) C; H: calcd, 5.52; found, 5.47, N: calcd, 5.48; found, 5.50.

***N*-2-(*p*-Chlorophenyl)ethylmaleamic Acid (25).** The mixture of maleic anhydride (256 mg, 2.62 mmol) and (*p*-chlorophenyl)ethylamine (340 mg, 2.19 mmol) in acetonitrile (30 mL) gave **25** (637 mg, 69%): ^{1}H NMR (DMSO-d_6, 300 MHz),

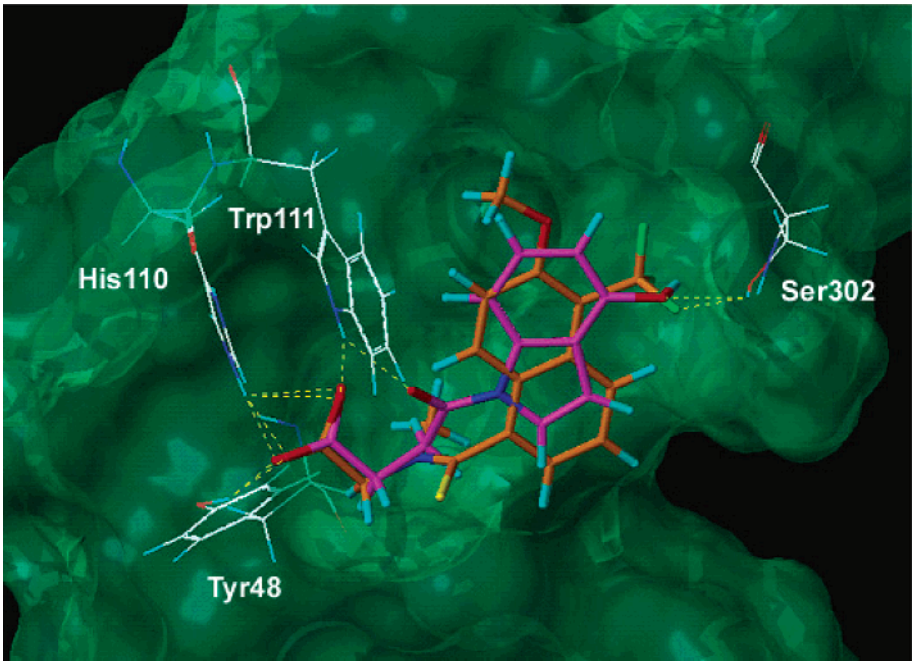

Figure 4. Superposition of the docked conformation of compound **46**, 4-oxo-4-(4-hydroxyindole)butanoic acid (magenta) with the experimentally obtained ALR2-bound conformation of tolrestat (orange). The connolly surface of the active site is shown in green, and the select residues which form hydrogen bonds with compound **46** or tolrestat are represented in line form. Hydrogen bonding interactions are shown in yellow dotted lines (<2.0 Å).

δ 7.33 (2H, d, Ar-*H*), δ 7.24 (2H, d, Ar-*H*), δ 6.34 (1H, t, COC*H* = CHCOOH), δ 6.20 (1H, t, COCH=C*H*COOH), δ 3.37 (2H, m, NHCH_2CH$_2$Ar), δ 2.75 (2H, t, NHCH$_2$CH_2Ar); ESI-MS *m*/*z* 253 (M^+). Anal. ($C_{12}H_{12}ClNO_3$) C; H: calcd, 4.77; found, 4.68, N: calcd, 5.52; found, 5.62.

***N*-2-(*p*-Chlorophenyl)ethylphthalamic Acid (26).** The mixture of phthalic anhydride (390 mg, 2.62 mmol) and (*p*-chlorophenyl)ethylamine (340 mg, 2.19 mmol) in acetonitrile (30 mL) gave **26** (607 mg, 55%): ^{1}H NMR (DMSO-d_6, 300 MHz) δ 8.38 (1H, t, N*H*CH$_2$CH$_2$Ar), δ 7.74 (2H, d, Ar-*H*), δ 7.56 (4H, m, CO*Ph*COOH), δ 7.35 (2H, m, Ar-*H*), δ 3.15 (2H, m, NHCH_2-CH$_2$Ar), δ 2.49 (2H, t, NHCH$_2$CH_2Ar); ESI-MS *m*/*z* 303 (M^+). Anal. ($C_{16}H_{14}ClNO_3$) C; H: calcd, 4.65; found, 4.56, N: calcd, 4.61; found, 4.58.

***N*-2-(*p*-Chlorophenyl)ethylglutaramic Acid (27).** The mixture of glutaric anhydride (299 mg, 2.62 mmol) and (*p*-chlorophenyl)ethylamine (340 mg, 2.19 mmol) in acetonitrile (30 mL) gave **27** (84 mg, 86%): ^{1}H NMR (DMSO-d_6, 300 MHz) δ 7.86 (1H, t, N*H*CH$_2$CH$_2$Ar), δ 7.31 (2H, m, Ar-*H*), δ 7.20 (2H, dd, Ar-*H*), δ 3.24 (2H, m, NHCH_2CH$_2$Ar), δ 2.66 (2H, t, NHCH$_2$CH_2Ar), δ 2.14 (2H, m, COCH_2CH$_2$CH$_2$COOH), δ 2.05 (2H, m, COCH$_2$CH$_2$CH_2COOH), δ 1.65 (2H, m, COCH$_2$CH_2-CH$_2$COOH); ESI-MS *m*/*z* 269 (M^+). Anal. ($C_{13}H_{16}ClNO_3$) C: calcd, 57.89; found, 57.44, H: calcd, 5.98; found, 6.01, N: calcd, 5.19; found, 5.08.

***N*-2-(*p*-Bromophenyl)ethylsuccinamic Acid (28).** The mixture of succinic anhydride (262 mg, 2.62 mmol) and (*p*-bromophenyl)ethylamine (437 mg, 2.19 mmol) in acetonitrile (30 mL) gave **28** (738 mg, 67%): ^{1}H NMR (DMSO-d_6, 300 MHz) δ 7.45 (2H, d, Ar-*H*), δ 7.15 (2H, d, Ar-*H*), δ 3.20 (2H, m, NHCH_2CH$_2$Ar), δ 2.64 (2H, t, NHCH$_2$CH_2Ar), δ 2.49 (2H, t, COCH_2CH$_2$COOH), δ 2.26 (2H, t, COCH$_2$CH_2COOH); ESI-MS *m*/*z* 300 (M^+). Anal. ($C_{12}H_{14}BrNO_3$) C, N; H: calcd, 6.33; found, 6.43.

***N*-2-(*p*-Bromophenyl)ethylmaleamic Acid (29).** The mixture of maleic anhydride (256 mg, 2.62 mmol) and (*p*-bromophenyl)ethylamine (437 mg, 2.19 mmol) in acetonitrile (30 mL) gave **29** (543 mg, 50%): ^{1}H NMR (DMSO-d_6, 300 MHz), δ 7.47 (2H, d, Ar-*H*), δ 7.18 (2H, d, Ar-*H*), δ 6.35 (1H, t, COC*H* = CHCOOH), δ 6.21 (1H, t, COCH=C*H*COOH), δ 3.16 (2H, m, NHCH_2CH$_2$Ar), δ 2.74 (2H, t, NHCH$_2$CH_2Ar); ESI-MS *m*/*z* 298 (M^+). Anal. ($C_{12}H_{12}BrNO_3$) C, N; H: calcd, 4.06; found, 4.02.

***N*-2-(*p*-Bromophenyl)ethylphthalamic Acid (30).** The mixture of phthalic anhydride (390 mg, 2.62 mmol) and (*p*-bromophenyl)ethylamine (437 mg, 2.19 mmol) in acetonitrile (30 mL) gave **30** (686 mg, 54%): ^{1}H NMR (DMSO-d_6, 300 MHz) δ 7.73 (1H, d, Ar-*H*), δ 7.54 (4H, s, CO*Ph*COOH), δ 7.30 (1H, d, Ar-*H*), δ 7.22 (2H, d, Ar-*H*), δ 3.14 (2H, m, NHCH_2CH$_2$Ar), δ 2.77 (2H, t, NHCH$_2$CH_2Ar); ESI-MS *m*/*z* 348 (M^+). Anal. ($C_{16}H_{14}BrNO_3$) C; H: calcd, 4.05; found, 3.97, N: calcd, 4.02; found, 3.98.

***N*-2-(*p*-Bromophenyl)ethylglutaramic Acid (31).** The mixture of glutaric anhydride (299 mg, 2.62 mmol) and (*p*-bromophenyl)ethylamine (437 mg, 2.19 mmol) in acetonitrile (30 mL) gave **31** (920 mg, 80%): ^{1}H NMR (DMSO-d_6, 300 MHz) δ 7.44 (2H, d, Ar-*H*), δ 7.14 (2H, m, Ar-*H*), δ 3.20 (2H, m, NHCH_2CH$_2$Ar), δ 2.62 (2H, t, NHCH$_2$CH_2Ar), δ 2.15 (2H, m, COCH_2CH$_2$CH$_2$COOH), δ 2.03 (2H, m, COCH$_2$CH$_2$CH_2COOH), δ 1.66 (2H, m, COCH$_2$CH_2CH$_2$COOH); ESI-MS *m*/*z* 314 (M^+). Anal. ($C_{13}H_{16}BrNO_3$) C, N; H: calcd, 5.13; found, 5.08.

***N*-Phenylsuccinamic Acid (32).** The mixture of succinic anhydride (262 mg, 2.62 mmol) and aniline (203 mg, 2.19 mmol) in acetonitrile (30 mL) gave **32** (149 mg, 21%): ^{1}H NMR (DMSO-d_6, 300 MHz) δ 9.92 (1H, s, N*H*Ar), δ 7.58 (2H, d, Ar-*H*), δ 7.28 (2H, t, Ar-*H*), δ 7.0 (1H, m, Ar-*H*), δ 2.57 (4H, br, COCH$_2$CH_2COOH); ESI-MS *m*/*z* 193 (M^+). Anal. ($C_{10}H_{11}NO_3$) C, N; H: calcd, 5.74; found, 5.70.

***N*-Phenylmaleamic Acid (33).** The mixture of maleic anhydride (256 mg, 2.62 mmol) and aniline (203 mg, 2.19 mmol) in acetonitrile (30 mL) gave **33** (605 mg, 87%): ^{1}H NMR (DMSO-d_6, 300 MHz) δ 10.38 (1H, s, N*H*Ar), δ 7.62 (2H, d, Ar-*H*), δ 7.32 (2H, m, Ar-*H*), δ 7.08 (H, t, Ar-*H*), δ 6.47 (1H, d, COC*H* = CHCOOH), δ 6.3 (1H, d, COCH=C*H*COOH); ESI-MS *m*/*z* 191 (M^+). Anal. ($C_{10}H_9NO_3$) C, N; H: calcd, 4.74; found, 4.68.

***N*-Phenylphthalamic Acid (34).** The mixture of phthalic anhydride (390 mg, 2.62 mmol) and aniline (203 mg, 2.19 mmol) in acetonitrile (30 mL) gave **34** (316 mg, 36%): ^{1}H NMR (DMSO-d_6, 300 MHz) δ 10.3 (1H, s, N*H*Ar), δ 7.91 (1H, d, CO*Ph*COOH), δ 7.62 (2H, m, CO*Ph*COOH), δ 7.6 (1H, m, Ar-*H*), δ 7.59 (2H, d, Ar-*H*), δ 7.3 (2H, d, Ar-*H*), δ 7.05 (1H, d, CO*Ph*COOH); ESI-MS *m*/*z* 241 (M^+). Anal. ($C_{14}H_{11}NO_3$) C, N; H: calcd, 4.60; found, 4.53.

***N*-Phenylglutaramic Acid (35).** The mixture of glutaric anhydride (299 mg, 2.62 mmol) and aniline (203 mg, 2.19

mmol) in acetonitrile (30 mL) gave **35** (257 mg, 34%): ^{1}H NMR (DMSO-d_6, 300 MHz) δ 9.86 (1H, s, NHAr), δ 7.58 (2H, d, Ar-*H*), δ 7.3 (2H, t, Ar-*H*), δ 6.98 (H, dd, Ar-*H*), δ 2.23 (4H, m, COCH_2CH$_2$CH_2COOH), δ 1.81 (2H, m, COCH$_2$CH_2CH$_2$COOH); ESI-MS *m*/*z* 207 (M^+). Anal. ($C_{11}H_{13}NO_3$) C, H; N: calcd, 6.33; found, 6.43.

***N*-Benzylsuccinamic Acid (36).** The mixture of succinic anhydride (262 mg, 2.62 mmol) and benzylamine (234 mg, 2.19 mmol) in acetonitrile (30 mL) gave **36** (172 mg, 23%): ^{1}H NMR (DMSO-d_6, 300 MHz) δ 8.35 (1H, s, N*H*CH$_2$Ar), δ 7.32 (3H, d, Ar-*H*), δ 7.21 (2H, d, Ar-*H*), δ 4.25 (2H, d, NHCH_2Ar), δ 2.44 (2H, t, COCH_2CH$_2$COOH), δ 2.39 (2H, t, COCH$_2$CH_2COOH); ESI-MS *m*/*z* 207 (M^+). Anal. ($C_{11}H_{13}NO_3$) C, H; N: calcd, 6.33; found, 6.43.

***N*-Benzylmaleamic Acid (37).** The mixture of maleic anhydride (256 mg, 2.62 mmol) and benzylamine (234 mg, 2.19 mmol) in acetonitrile (30 mL) gave **37** (203 mg, 27%): ^{1}H NMR (DMSO-d_6, 300 MHz) δ 9.39 (1H, s, N*H*CH$_2$Ar), δ 7.34 (5H, m, Ar-*H*), δ 6.44 (1H, d, COC*H* = CHCOOH), δ 6.26 (1H, d, COCH=C*H*COOH), δ 4.39 (2H, d, NHCH_2Ar); ESI-MS *m*/*z* 205 (M^+). Anal. ($C_{11}H_{11}NO_3$) C, H; N: calcd, 6.33; found, 6.43.

***N*-Benzylphthalamic Acid (38).** The mixture of phthalic anhydride (390 mg, 2.62 mmol) and benzylamine (234 mg, 2.19 mmol) in acetonitrile (30 mL) gave **38** (259 mg, 28%): ^{1}H NMR (DMSO-d_6, 300 MHz) δ 8.83 (1H, s, N*H*CH$_2$Ar), δ 7.76 (1H, s, CO*Ph*COOH), δ 7.5 (2H, m, CO*Ph*COOH), δ 7.3 (5H, br, Ar-*H*), δ 7.2 (1H, d, CO*Ph*COOH), δ 4.43 (2H, d, NHCH_2Ar); ESI-MS *m*/*z* 255 (M^+). Anal. ($C_{15}H_{13}NO_3$) C, N, H: calcd, 5.13; found, 5.08.

***N*-Benzylglutaramic Acid (39).** The mixture of glutaric anhydride (299 mg, 2.62 mmol) and benzylamine (234 mg, 2.19 mmol) in acetonitrile (30 mL) gave **39** (123 mg, 16%): ^{1}H NMR (DMSO-d_6, 300 MHz) δ 8.32 (1H, s, N*H*CH$_2$Ar), δ 7.29 (3H, m, Ar-*H*), δ 7.22 (2H, dd, Ar-*H*), δ 4.24 (2H, d, NHCH_2Ar), δ 2.2 (4H, m, COCH_2CH$_2$CH_2COOH), δ 1.7 (2H, m, COCH$_2$CH_2-CH$_2$COOH); ESI-MS *m*/*z* 221 (M^+). Anal. ($C_{12}H_{15}NO_3$) C, H; N: calcd, 6.33; found, 6.36.

4-Oxo-4-(2,3-dihydroindole)butanoic Acid (40). The mixture of succinic anhydride (262 mg, 2.62 mmol), indoline (260 mg, 2.19 mmol) and TEA (3 mL, 21.87 mmol) in acetonitrile (30 mL) gave **40** (171 mg, 21%): ^{1}H NMR (DMSO-d_6, 300 MHz), δ 12.09 (1H, s, COCH$_2$CH$_2$COO*H*), δ 8.04 (1H, d, NCC*H* = CHCH=CH), δ 7.22 (1H, dd, NCCH=CHC*H* = CH), δ 7.13 (1H, dd, NCCH=C*H*CH=CH), δ 6.97 (1H, t, NCCH=CHCH=C*H*), δ 4.09 (2H, t, NCH_2CH$_2$), δ 3.14 (2H, t, NCH$_2$CH_2), δ 2.67 (2H, t, COCH_2CH$_2$COOH), δ 2.51 (2H, t, COCH$_2$CH_2-COOH); ESI-MS *m*/*z* 219 (M^+). Anal. ($C_{12}H_{13}NO_3$) C, H; N: calcd, 6.33; found, 6.43.

4-Oxo-4-(2,3-dihydroindole)-*cis*-2-buteneoic Acid (41). The mixture of maleic anhydride (256 mg, 2.62 mmol), indoline (260 mg, 2.19 mmol) and TEA (3 mL, 21.87 mmol) in acetonitrile (30 mL) gave **41** (318 mg, 40%): ^{1}H NMR (DMSO-d_6, 300 MHz), δ 12.8 (1H, s, COCH=CHCOO*H*), δ 8.03 (1H, d, NCC*H* = CHCH=CH), δ 7.24 (2H, m, NCCH=C*H*C*H* = CH), δ 7.18 (1H, dd, NCCH=CHCH=C*H*), δ 7.90 (1H, d, COC*H* = CHCOOH), δ 6.12 (1H, d, COCH=C*H*COOH), δ 3.98 (2H, t, NCH_2CH$_2$), δ 3.1 (2H, t, NCH$_2$CH_2); ESI-MS *m*/*z* 217 (M^+). Anal. ($C_{12}H_{11}NO_3$) C, N; H: calcd, 5.10; found, 5.15.

5-Oxo-5-(2,3-dihydroindole)pentanoic Acid (42). The mixture of glutaric anhydride (299 mg, 2.62 mmol), indoline (260 mg, 2.19 mmol) and TEA (3 mL, 21.87 mmol) in acetonitrile (30 mL) gave **42** (211 mg, 25%): ^{1}H NMR (DMSO-d_6, 300 MHz) δ 8.04 (1H, d, NCC*H*=CHCH=CH), δ 7.20 (1H, m, NCCH=C*H*CH=CH), δ 7.71 (1H, m, NCCH=CHC*H* = CH), δ 6.95 (1H, dd, NCCH=CHCH=C*H*), δ 4.03 (2H, t, NCH_2CH$_2$), δ 3.11 (2H, t, NCH$_2$CH_2), δ 2.48 (2H, t, COCH_2CH$_2$CH$_2$COOH), δ 2.29 (2H, t, COCH$_2$CH$_2$CH_2COOH), δ 1.78 (2H, t, COCH$_2$CH_2-CH$_2$COOH); ESI-MS *m*/*z* 233 (M^+). Anal. ($C_{13}H_{15}NO_3$) H; C: calcd, 66.94; found, 67.52, N: calcd, 6.00; found, 6.11.

4-Oxo-4-indolebutanoic Acid (43). The mixture of succinic anhydride (262 mg, 2.62 mmol), indole (256 mg, 2.19 mmol) and TEA (3 mL, 21.87 mmol) in acetonitrile (30 mL) gave **43** (198 mg, 25%): ^{1}H NMR (DMSO-d_6, 300 MHz), δ 12.26 (1H, s, COCH$_2$CH$_2$COO*H*), δ 8.33 (1H, d, NCCH=CHCH=C*H*), δ 7.93 (1H, d, NCC*H* = CHCH=CH), δ 7.63 (1H, dd, NCCH=C*H*CH=CH), δ 7.32 (1H, d, NC*H* = CH), δ 7.25 (1H, d, NCH=C*H*), δ 6.76 (1H, m, NCCH=CHC*H* = CH), δ 3.25 (2H, t, COCH_2CH$_2$COOH), δ 2.66 (2H, t, COCH$_2$CH_2COOH); ESI-MS *m*/*z* 217 (M^+). Anal. ($C_{12}H_{11}NO_3$) C, H; N: calcd, 6.45; found, 6.36.

4-Oxo-4-indole-*cis*-2-buteneoic Acid (44). The mixture of maleic anhydride (256 mg, 2.62 mmol), indole (256 mg, 2.19 mmol) and TEA (3 mL, 21.87 mmol) in acetonitrile (30 mL) gave **44** (144 mg, 18%): ^{1}H NMR (DMSO-d_6, 300 MHz), δ 12.26 (1H, s, COCH$_2$CH$_2$COO*H*), δ 8.33 (1H, d, NCCH=CHCH=C*H*), δ 7.93 (1H, d, NCC*H* = CHCH=CH), δ 7.63 (1H, dd, NCCH=C*H*CH=CH), δ 7.32 (1H, d, NC*H* = CH), δ 7.25 (1H, d, NCH=C*H*), δ 6.76 (1H, m, NCCH=CHC*H* = CH), δ 6.45 (1H, d, COC*H* = CHCOOH), δ 6.33 (1H, d, COCH=C*H*COOH); ESI-MS *m*/*z* 215 (M^+). Anal. ($C_{12}H_9NO_3$) C: calcd, 66.97; found, 57.38, H: calcd, 4.22; found, 4.39, N: calcd, 6.51; found, 5.31.

5-Oxo-5-indolepentanoic Acid (45). The mixture of glutaric anhydride (299 mg, 2.62 mmol), indole (256 mg, 2.19 mmol) and TEA (3 mL, 21.87 mmol) in acetonitrile (30 mL) gave **45** (471 mg, 56%): ^{1}H NMR (DMSO-d_6, 300 MHz), δ 8.33 (1H, d, NCCH=CHCH=C*H*), δ 7.86 (1H, d, NCC*H* = CHCH=CH), δ 7.60 (1H, dd, NCCH=C*H*CH=CH), δ 7.30 (1H, d, NC*H* = CH), δ 7.24 (1H, d, NCH=C*H*), δ 6.73 (1H, m, NCCH=CHC*H* = CH), δ 3.04 (2H, t, COCH_2CH$_2$CH$_2$COOH), δ 2.36 (2H, t, COCH$_2$CH$_2$CH_2COOH), δ 1.90 (2H, t, COCH$_2$CH_2CH$_2$-COOH); ESI-MS *m*/*z* 231 (M^+). Anal. ($C_{13}H_{13}NO_3$) H; C: calcd, 67.52, found, 68.31, N: calcd, 6.06; found, 6.21.

4-Oxo-4-(4-hydroxyindole)butanoic Acid (46). The mixture of succinic anhydride (262 mg, 2.62 mmol), 4-hydroxyindole (291 mg, 2.19 mmol) and TEA (3 mL, 21.87 mmol) in acetonitrile (30 mL) gave **46** (300 mg, 33%): ^{1}H NMR (DMSO-d_6, 300 MHz), δ 7.80 (1H, d, NCC*H* = CHCH=CH), δ 7.77 (1H, d, NCCH=CHC*H* = CH), δ 7.10 (1H, m, NC*H* = CH), δ 6.78 (1H, dd, NCCH=C*H*CH=CH), δ 6.65 (1H, d, NCH=C*H*), δ 3.22 (2H, t, COCH_2CH$_2$COOH), δ 2.62 (2H, t, COCH$_2$CH_2COOH); ESI-MS *m*/*z* 233 (M^+). Anal. ($C_{12}H_{11}NO_4$) H; C: calcd, 61.80; found, 61.20, N: calcd, 6.01; found, 5.87.

Flexible Docking. The structures of the ligands were prepared in MOL2 format using the sketcher module of Sybyl 6.8[47] and Gasteiger−Huckel charges were assigned to the ligand atoms. The minimization was run until converged to a maximum derivative of 0.001 kcal mol^{-1} Å^{-1}, and the final coordinates were stored in database. The X-ray crystal structure of porcine ALR2 complexed with NADP$^+$ and tolrestat (pdb entry = 1AH3) were retrieved from the Protein Data Bank (PDB). The active site was defined as all the amino acid residues enclosed within 6.5 Å radius sphere centered by the bound ligand, tolrestat. The docking and subsequent scoring were performed using the default parameters of the FlexX program implanted in the Sybyl 6. 8. For the docking of the ligand library into the target active site, the main settings are 1000 solutions per iteration during the incremental construction algorithm and a maximum protein−ligand atom−atom overlap of 2.5 Å^3. Final scores for all FlexX solutions (up to 1000) per compound were calculated by consensus scoring program, Cscore, and used for database ranking.

3D QSAR. Hydrophobic, donor, and acceptor fields were calculated with CoMSIA (Comparative Molecular Field Analysis) module integrated in SYBYL 6.8. For building the pseudo receptor, the hydrogen bond donor, the hydrogen bond acceptor, and the hydrophobic fields are considered. An sp^3 carbon atom with a +1.0 charge was selected as a probe for the calculation of hydrophobic, donor, and acceptor, filtered at 8 kcal/mol. The FlexX-docked alignment of top-scoring conformations was used for 3D QSAR analysis.

References

(1) Pfeifer, M. A.; Schumer, M. P. Clinical trials of diabetic neuropathy: Past, present, and future. *Diabetes* **1995**, *44*, 1355−1361.

(2) Williamson, J. R.; Ostrow, E.; Eades, D.; Chang, K.; Allison, W.; Kilo, C.; Sherman, W. R. Glucose-induced microvascular functional changes in nondiabetic rats are stereospecific and are prevented by an aldose reductase inhibitor. *J. Clin. Invest.* **1990**, *85*, 1167−1172.

(3) Maragoudakis, M. E.; Wasvary, J.; Hankin, H.; Gargiulo, P. Human placenta aldose reductase: Forms sensitive and insensitive to inhibition by alrestatin. *Mol. Pharmacol.* **1984**, *25*, 425−430.
(4) Kotani, T.; Nagaki, Y.; Ishii, A.; Konishi, Y.; Yaho, H.; Suehiro, S.; Okukado, N.; Okamoto, K. Highly selective aldose reductase inhibitors. 3. Structural diversity of 3-(arylmethyl)-2,4,5-trioxoimidazolidine-1-acetic acids. *J. Med. Chem.* **1997**, *40*, 684−694.
(5) Costantino, L.; Rastelli, G.; Gamberini, M. C.; Vinson, J. A.; Bose, P.; Iannone, A.; Staffieri, M.; Antolini, L.; Del Corso, A.; Mura, U.; Albasini, A. 1-Benzopyran-4-one antioxidants as aldose reductase inhibitors. *J. Med. Chem.* **1999**, *42*, 1881−1893.
(6) Kurono, M.; Fujiwara, I.; Yoshida, K. Stereospecific interaction of a novel spirosuccinimide type aldose reductase inhibitor, AS-3201, with aldose reductase. *Biochemistry* **2001**, *40*, 8216−8226.
(7) Kawamura, M.; Hamanaka, N. Development of Eparlestat (Kinedak), aldose reductase inhibitor. *J. Synth. Org. Chem.* **1997**, *37*, 787−792.
(8) Costantino, L.; Rastelli, G.; Vescovini, K.; Cignarella, G.; Vianello, P.; Del Corso, A.; Cappiello, M.; Mura, U.; Barlocco, D. Synthesis, activity, and molecular modeling of a new series of tricyclic pyridazinones as selective aldose reductase inhibitors. *J. Med. Chem.* **1996**, *39*, 4396−4405.
(9) Fresneau, P.; Cussac, M.; Morand, J. M.; Szymonski, B.; Tranqui, D.; Leclerc, G. Synthesis, activity, and molecular modeling of new 2,4-dioxo-5-(naphthylene)-3-thiazolidineacetic acids and 2-thioxo analogues as potent aldose reductase inhibitors. *J. Med. Chem.* **1998**, *41*, 4706−4715.
(10) Harrison, D. H.; Bohren, K. M.; Petsko, G. A.; Ringe, D.; Gabbay, K. H. The alrestatin double-decker: binding of two inhibitor molecules to human aldose reductase reveals a new specificity determinant. *Biochemistry* **1997**, *36*, 16134−16140.
(11) Yabe-Nishimura, C. Aldose reductase in glucose toxicity: A potential target for the prevention of diabetic complications. *Pharmacol. Rev.* **1998**, *50*, 21−33.
(12) El-Kabbani, O.; Carper, D. A.; McGowan, M. H.; Devedjiev, Y.; Rees-Milton, K. J.; Flynn, T. G. Studies on the inhibitor-binding site of porcine aldehyde reductase: Crystal structure of the holoenzyme−inhibitor ternary complex. *Proteins* **1997**, *29*, 186−192.
(13) Nakano, T.; Petrash, J. M. Kinetic and spectroscopic evidence for active site inhibition of human aldose reductase. *Biochemistry* **1996**, *35*, 11196−11202.
(14) Varnai, P.; Warshel, A. Computer simulation studies of the catalytic mechanism of human aldose reductase. *J. Am. Chem. Soc.* **2000**, *122*, 3849−3860.
(15) Rastelli, G.; Vianello, P.; Barlocco, D.; Costantino, L.; Corso, A. D.; Mura, U. Structure-based design of an inhibitor modeled at the substrate active site of aldose reductase. *Bioorg. Med. Chem. Lett.* **1997**, *7*, 1897−1902.
(16) Singh, S. B.; Malamas, M. S.; Hohman, T. C.; Nilakantan, R.; Carper, D. A.; Kitchen, D. Molecular modeling of the aldose reductase-inhibitor complex based on the X-ray crystal structure and studies with single-site-directed mutants. *J. Med. Chem.* **2000**, *43*, 1062−1070.
(17) Gane, P. J.; Dean, P. M. Recent advances in structure-based rational drug design. *Curr. Opin. Struct. Biol.* **2000**, *10*, 401−404.
(18) Joseph-McCarthy, D. Computational approaches to structure-based ligand design. *Pharmacol. Ther.* **1999**, *84*, 179−191.
(19) Makara, G. M. Measuring Molecular Similarity and Diversity: Total Pharmacophore Diversity. *J. Med. Chem.* **2001**, *44*, 3563−3571.
(20) Muegge, I.; Martin, Y. C. A general and fast scoring function for protein−ligand interactions: a simplified potential approach. *J. Med. Chem.* **1999**, *42*, 791−804.
(21) Stahl, M.; Rarey, M. Detailed analysis of scoring function for virtual screening. *J. Med. Chem.* **2001**, *44*, 1035−1042.
(22) Walters, W. P.; Stahl, M. T.; Murcko, M. A. Virtual screening-An overview. *Drug Discovery Today* **1998**, *3*, 160−178.
(23) Good, A. C.; Krystek, S. R.; Mason, J. S. High-throughput and virtual screening: core lead discovery technologies move towards integration. *Drug Discovery Today* **2000**, *5*, 561−569.
(24) Bissantz, C.; Folkers, G.; Rognan, D. Protein-based virtual screening of chemical database. 1. Evaluation of different docking/scoring combinations. *J. Med. Chem.* **2000**, *43*, 4759−4767.
(25) Costantino, L.; Corso, A. D.; Rastelli, G.; Petrash, J. M.; Mura, U. 7-Hydroxy-2-substituted-4-*H*-1-benzopyran-4-one derivatives as aldose reductase inhibitors: a SAR study. *Eur. J. Med. Chem.* **2001**, *36*, 697−703.
(26) Costantino, L.; Rastelli, G.; Gamberini, M. C.; Vinson, J. A.; Bose, P.; Iannone, A.; Staffieri, M.; Antolini, L.; Del Corso, A.; Mura, U.; Albasini, A. 1-Benzopyran-4-one antioxidants as aldose reductase inhibitors. *J. Med. Chem.* **1999**, *42*, 1881−1893.
(27) Rastelli, G.; Ferrari, A. M.; Costantino, L.; Gamberini, M. C. Discovery of new inhibitors of aldose reductase from molecular docking and database screening. *Bioorg. Med. Chem.* **2002**, *10*, 1437−1450.
(28) Iwata, Y.; Arisawa, M.; Hamada, R.; Kita, Y.; Mizutani, M. Y.; Tomioka, N.; Itai, A.; Miyamoto, S. Discovery of novel aldose reductase inhibitors using a protein structure-based approach: 3D-database search followed by design and synthesis. *J. Med. Chem.* **2001**, *44*, 1718−1728.
(29) Bahn, Y. S.; Park, J. M.; Bai, D. H.; Takase, S.; Yu, J. H. YUA001, a novel aldose reductase inhibitor isolated from alkalophilic *Corynebacterium* sp. YUA25: I. taxonomy, fermentation, isolation and characterization. *J. Antibiotics* **1998**, *10*, 902−907.
(30) Claussen, H.; Buning, C.; Rarey, M.; Lengauer, T. FlexE: Efficient molecular docking considering protein structure variations. *J. Mol. Biol.* **2001**, *308*, 377−395.
(31) Suh, M. E.; Kang, M. J.; Park, S. Y. The 3-D QSAR study of anticancer 1-*N*-substituted imidazo- and pyrrolo-quinoline-4,9-dione derivatives by CoMFA and CoMSIA. *Bioorg. Med. Chem.* **2001**, *9*, 2987−2991.
(32) Cavalli, A.; Greco, G.; Novellino, E.; Recanatini, M. Linking CoMFA and protein homology models of enzyme−inhibitor interactions: an Application to nonsteroidal aromatase inhibitors. *Bioorg. Med. Chem.* **2000**, *8*, 2771−2780.
(33) Liu, H.; Ji, M.; Jiang, H.; Liu, L.; Hua, W.; Chen, K.; Ji, R. Computer-aided design, synthesis and biological assay of *p*-methylsulfonamido phenylethylamine analogues. *Bioorg. Med. Chem. Lett.* **2000**, *10*, 2153−2157.
(34) Sun, W. S.; Lee, H. S.; Park, J. M.; Kim, S. H.; Yu, J. H.; Kim, J. H. YUA001, a novel aldose reductase inhibitor isolated from alkalophilic *corynebacterium* sp. YUA25 II. Chemical modification and biological activity. *J. Antibiot.* **2001**, *54*, 827−830.
(35) Mohri, K.; Suzuku, K.; Usui, M.; Isobe, K.; Tsuda, Y. Convenient synthesis of tertiary amines by alkylation of secondary amines with alkyl halides in the presence of potassium hydride and triethylamine. *Chem. Pharm. Bull.* **1995**, *43*, 159−161.
(36) Rarey, M.; Kramer, B.; Lengauer, T.; Klebe, G. A fast flexible docking method using an incremental construction algorithm. *J. Mol. Biol.* **1996**, *261*, 470−489.
(37) Kramer, B.; Rarey, M.; Lengauer, T. Evaluation of the FLEXX incremental construction algorithm for protein−ligand docking. *Proteins* **1999**, *37*, 228−241.
(38) Urzhumtsev, A.; Tete, F. A.; Mitschler, A.; Barbanton, J.; Barth, P.; Urzhumtseva, L.; Biellmann, J. F.; Podjarny, A.; Moras, D. A specificity pocket inferred from the crystal structures of the complexes of aldose reductase with the pharmaceutically important inhibitors tolrestat and sorbinil. *Structure* **1997**, *5*, 601−612.
(39) Meng, E. C.; Shoichet, B. K.; Kuntz, I. D. Automated docking with grid-based energy evaluation. *J. Comput. Chem.* **1992**, *13*, 505−524.
(40) Knegtel, R. M.; Bayada, D. M.; Engh, R. A.; von der Saal, W.; van Geerestein, V. J.; Grootenhuis, P. D. Comparison of two implementations of the incremental construction algorithm in flexible docking of thrombin inhibitors. *J. Comput.-Aid. Mol. Des.* **1999**, *13*, 167−183.
(41) Eldridge, M. D.; Murray, C. W.; Auton, T. R.; Paolini, G. V.; Mee, R. P. Empirical scoring functions: I. The development of a fast empirical scoring function to estimate the binding affinity of ligands in receptor complexes *J. Computer-Aided Mol. Des.* **1997**, *11*, 425−445.
(42) Bernstein, F. C.; Koetzle, T. F.; Williams, G. J.; Meyer, E. F. Jr; Brice, M. D.; Rodgers, J. R.; Kennard, O.; Shimanouchi, T.; Tasumi, M. The Protein Data Bank. A computer-based archival file for macromolecular structures. *Eur. J. Biochem.* **1977**, *80*, 319−324.
(43) Cramer, R. D. III; Patterson, D. E.; Bunce, J. D.; Comparative molecular field analysis (CoMFA). 1. Effect of shape on binding of steroids to carrier proteins. *J. Am. Chem. Soc.* **1988**, *110*, 5959−5967.
(44) Klebe, G.; Abraham, U.; Mietzner, T. Molecular similarity indices in a comparative analysis (CoMSIA) of drug molecules to correlate and predict their biological activity. *J. Med. Chem.* **1994**, *37*, 4130−4146.
(45) Klebe, G.; Abraham, U. Comparative molecular similarity index analysis (CoMSIA) to study hydrogen-bonding properties and to score combinatorial libraries. *J. Comput.-Aided Mol. Des.* **1999**, *13*, 1−10.
(46) Sippl, W.; Höltje, H.-D. Structure-based 3D-QSAR-merging the accuracy of structure-based alignment with the computational efficiency of ligand-based methods. *Journal of Molecular Structure: Theochem* **2000**, *503*, 31−50.
(47) *Sybyl*, 6.8 ed.; SYBYL molecular modeling software, Tripos Inc.: St. Louis, MO, **2000**.

JM0205346